Co-funded by the European Union

Research Fund for Coal & Steel

Hybrid energy storage system using post-mining infrastructure (HESS)

Deliverable 4.2

Guidelines for the baseline condition of the reference shafts

31.12.2025

PROJECT	
Project number	**101112380**
Project name	**Hybrid energy storage system using post-mining infrastructure**
Project acronym:	**HESS**
Call	**RFCS-2022**
Topic	**RFCS-01-2022-RPJ**
Type of action	**RFCS-PJG**
Service	**REA/B/01**

DOCUMENT PROPERTIES

Document Number	**D.4.2**
Document Title	**Guidelines for the baseline condition of the reference shafts**
Document responsible	**SUT**
Target dissemination level	**PU**
Document authors	**Grzegorz Smolnik (SUT)** **Konrad Kołodziej (SUT)** **Marcin Lutyński (SUT)**
Data of the document	**31.12.2025**

Table of contents

1. Introduction and Purpose

In the face of the global energy transition and the necessity of balancing unstable renewable energy sources, the HESS project (Hybrid Energy Storage System) undertakes the challenge of revitalizing decommissioned coal infrastructure. The concept of adapting deep mine shafts into compressed air energy storage (CAES) reservoirs aligns with the principles of the circular economy, giving a "second life" to capital-intensive engineering structures that would otherwise be liquidated. Thanks to their unique geometry and depth, these shafts offer a natural advantage over surface pressure vessels; however, their adaptation involves specific risks resulting from long-term operation in difficult geological conditions.

This document, constituting Deliverable 4.2 (D4.2), defines the "Baseline Conditions" for reference shafts. It is a set of critical technical and geomechanical parameters that establish the safety limit for the future installation. The aim of this study is to translate general conceptual assumptions into precise engineering guidelines for a specific object - the “Budryk III” shaft. This document serves as a validation framework barrier: it defines the minimum standard of technical condition that the shaft must represent for its adaptation into a high-pressure compressed air reservoir to be admissible from the point of view of structural and rock mass safety.

1.1. Design Background and Implementation

The implementation of this study constitutes a logical continuation of a sequence of research works aimed at the implementation of CAES technology in post-mining shafts. The preliminary phases of the project (WP2) enabled an inventory of the Upper Silesian Coal Basin Lublin Coal Basin, Czech Republic resources and the selection of objects with the highest adaptive potential. This process, based on multi-criteria analysis, allowed for the identification of locations meeting preliminary geometric and locational criteria, eliminating areas with unfavourable general conditions.

Parallel to the selection process, advanced numerical simulations were conducted within the framework of analytical works (WP3). Utilizing geomechanical models, the theoretical feasibility of loading shaft linings with cyclic internal pressure of the order of 8 MPa was verified. These studies allowed for the mapping of potential increased stress states in the rock mass and the identification of theoretical zones where the shaft structure may require special design attention.

The role of this document (D4.2) is to translate the results of these simulations for the needs of the reference object. This report constitutes a synthesis of theoretical knowledge and transfers it to the level of technical requirements for a specific engineering structure. The document defines the profile of geometric, structural, and strength parameters that are adopted as the baseline standard ("Baseline") for safe operation. Thus, these guidelines constitute a reference framework for assessing the compliance of existing infrastructure with the design assumptions of the energy storage system, ensuring consistency between the computational model and the actual mining facility

1.2. Selection and Characteristics of the Reference Shaft: Budryk III

In the process of selecting a reference object for defining Baseline Conditions, a key aspect was identifying a mine working that represents the highest technical and operational standard, while simultaneously guaranteeing the safety of the future pressure installation. Based on a multi-criteria analysis, the Budryk III (Fig.1) shaft was selected as the model object. It is a hoisting, material, and man-riding shaft, functioning as an air intake, which determines its strategic importance in the mine structure and the specificity of its massive construction. The decision to select this object is dictated by four key factors: geometry, unique lining structure, operational resilience, and hybridization potential.

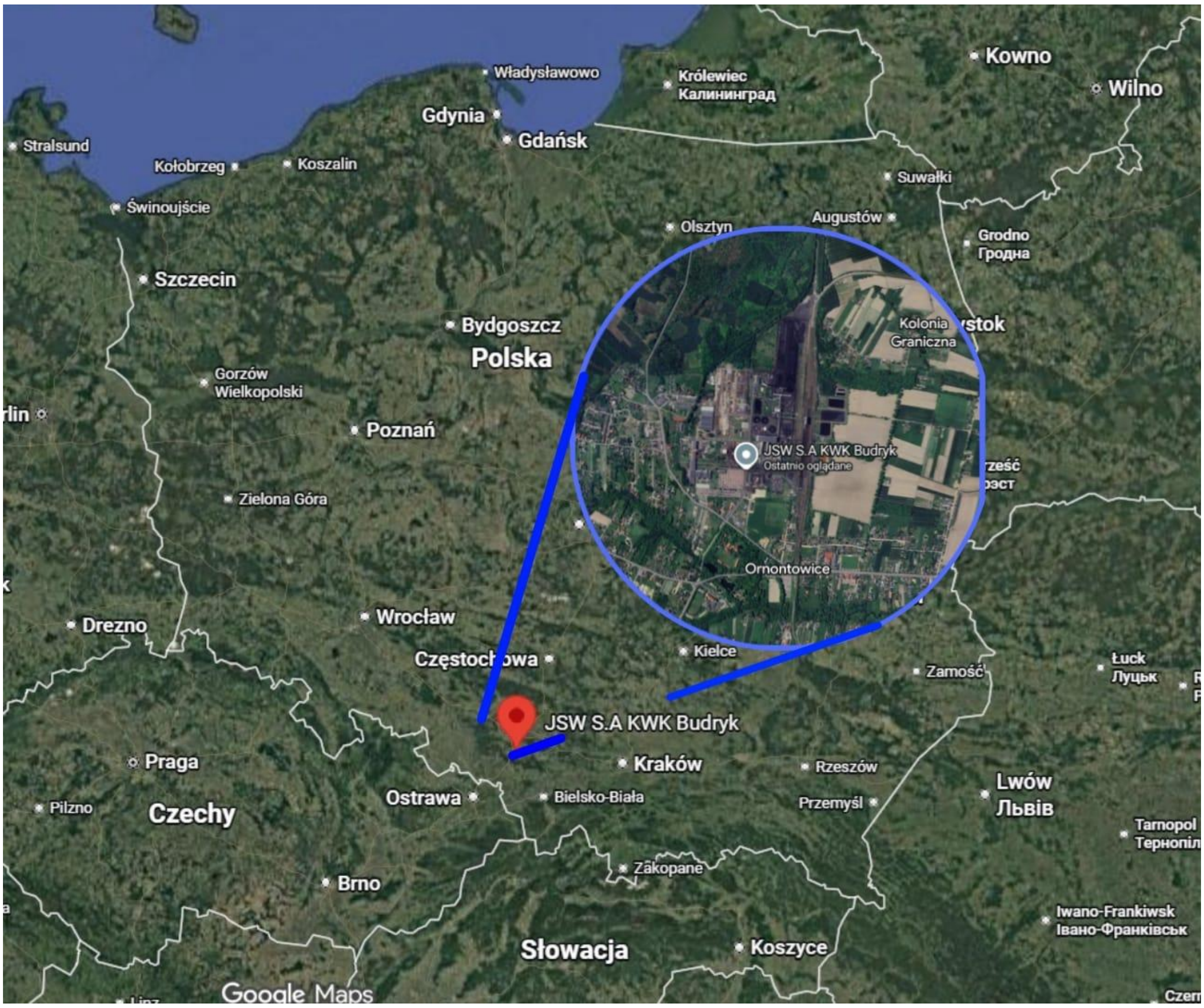

Figure 1 Localization of selected shaft.

The selection of the Budryk III shaft was supported by a Multi-Criteria Decision Analysis (MCDA), which enabled a structured and transparent comparison of candidate shafts using a consistent set of technical and operational criteria, as described in Deliverable 2.1. [1].

The analysis incorporated geometric parameters, structural characteristics of the shaft lining, current operational function, accessibility, and long-term adaptability to pressurised operation. By aggregating these criteria within a unified decision framework, MCDA allowed the identification of the shaft that best balances technical robustness with future adaptation potential, thereby providing a rational basis for defining a representative reference object for the development of Baseline Conditions.

1.2.1. Geometry Architecture and Parameters

The Budryk III shaft (Fig. 2) is characterized by parameters that ideally predispose it to the role of a large-scale, underground pressure reservoir:

- **Total depth:** 1090 m, which ensures vast active capacity in the vertical arrangement and the possibility of obtaining a high-pressure gradient.
- **Shaft diameter:** 9.0 m. This is one of the largest cross-sections in Polish mining.
- **Regular, circular cross-section** of such a large diameter is optimal for the distribution of stresses from internal pressure (so-called hoop stresses), minimizing the risk of local stress concentrations in the lining structure.

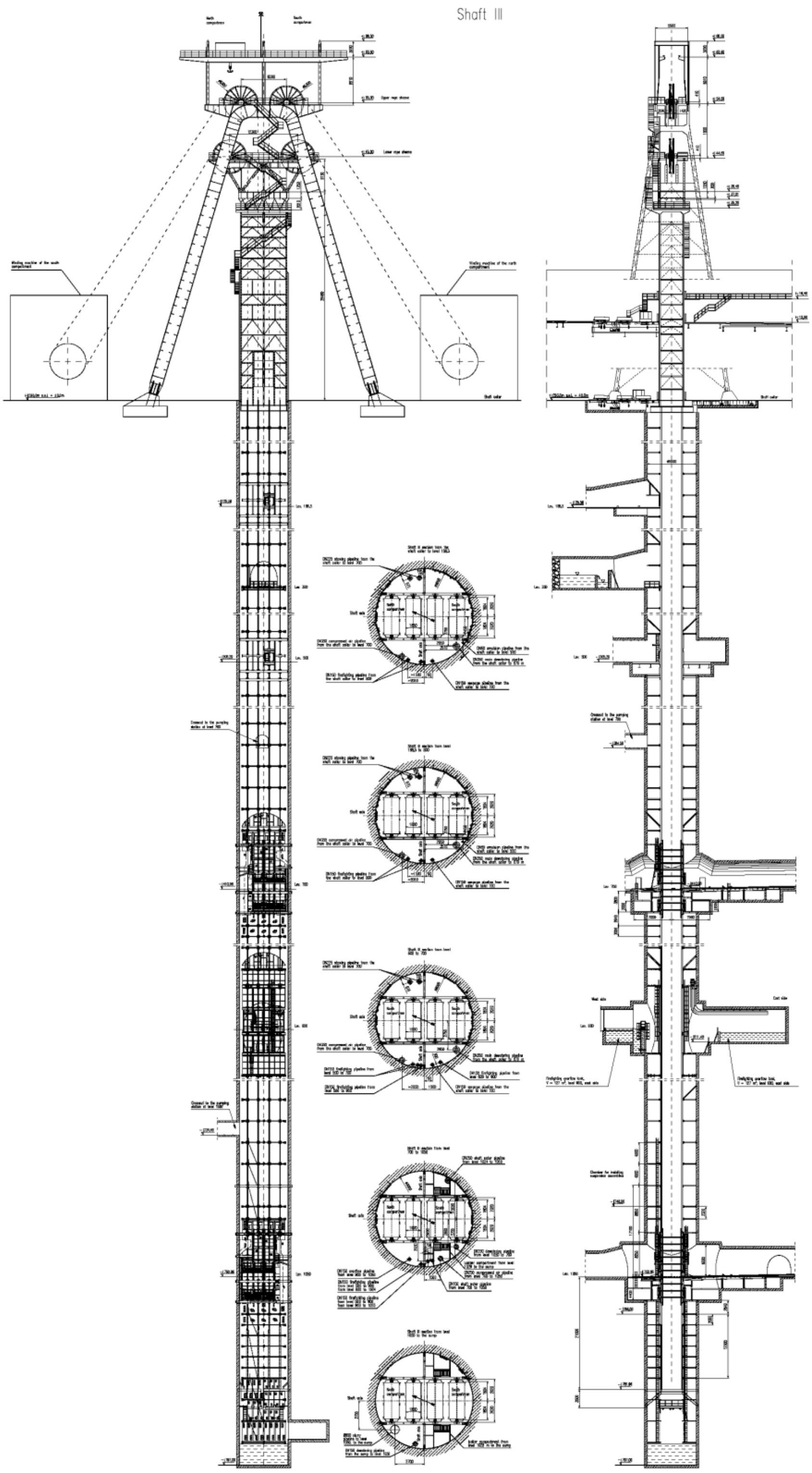

Figure 2 Schematic view of Shaft III Budryk mine.

1.2.2. Enclosure Profile and Structural Strength

The structure of the excavation support is based on a monolithic concrete lining of variable thickness, precisely adapted to local geological conditions. Analysis of the profile reveals the existence of zones of increased stiffness, which is crucial for the Baseline:

- **Foundations and Collar:** The shaft possesses extremely solid extremities. The shaft head (from the collar to a depth of 5.3 m) is made of concrete with a thickness of 1.5 m , and the shaft bottom is protected by a concrete footing of an analogous thickness of up to 1.5 m. These massive elements constitute natural, ready-made zones for anchoring the planned sealing plugs (upper and lower) of the CAES reservoir.
- **Shaft Barrel:** The base thickness of the single concrete lining ranges from 0.4 m to 0.5 m.
- **Reinforced Zones:** In areas where coal seams occur, where the rock mass shows tendencies towards convergence, the lining was systematically thickened to 0.75 m. Additionally, in selected sections, a composite lining (double: masonry and concrete) was applied with a total thickness reaching up to 0.88 m. Such a structure proves that the shaft was designed with a large safety margin regarding rock mass deformations.

1.2.3. Technology Nodes and Lining Discontinuities

Detailed inventory reveals the specificity of the shaft's connections with the horizontal infrastructure, which is critical for the tightness of the reservoir . The shaft possesses a series of insets, which can be divided into two categories:

- **Active Station (Double-sided/Single-sided):** Connections with mine workings (e.g., at levels 500 m, 700 m, 1050 m). They require the design of isolation dams capable of withstanding full operating pressure; the scheme for such works has been described in previous reports.
- **"Blind" Station and Tube Lunettes:** A significant asset are insets not connected to mine workings (e.g., at depths of 349.2 m, 900 m, 1085.1 m) and specific "tube lunettes" (at depths of 677.5 m and 1027.2 m). The presence of these elements, which do not require extensive damming (lack of an extensive network of workings behind them), simplifies the adaptation and sealing process.

1.2.4. Operational Reliability and Hydrogeological Conditions

A key argument supporting the selection of Shaft III is its proven operational resilience. This shaft, originally equipped with two powerful hoists with four-deck cages, has for years transferred enormous dynamic loads and vibrations associated with the transport of crew and materials. Its structure demonstrated stability, playing, among other things, a key logistical role during works related to the sinking of another shaft. The fact that the casing-maintained integrity in such a difficult operating regime is a strong predictor of its ability to transfer static loads from the compressed medium.

From a CAES perspective, favourable hydrogeological conditions are a critical asset. The shaft is a relatively dry facility, which is confirmed by the fact that its role in the drainage system was secondary. Low water infiltration from behind the lining minimizes the risk of chemical corrosion of the concrete and problems with the humidity of the stored air, which directly translates into the durability and energy efficiency of the entire storage facility.

1.2.5. Hybridization Potential (HESS Project)

The selection of Shaft III is inextricably linked to the concept of the HESS hybrid system. This shaft is located in close proximity to Shaft II (Fig. 3) (a ventilation shaft with a depth of 1158 m and a diameter of 9.0 m). This spatial proximity creates a unique synergy – a pair of shafts with similar geometric parameters allows for the design of an advanced system (e.g., dua l-reservoir or cooperative), which constitutes the foundation of the entire project's innovation.

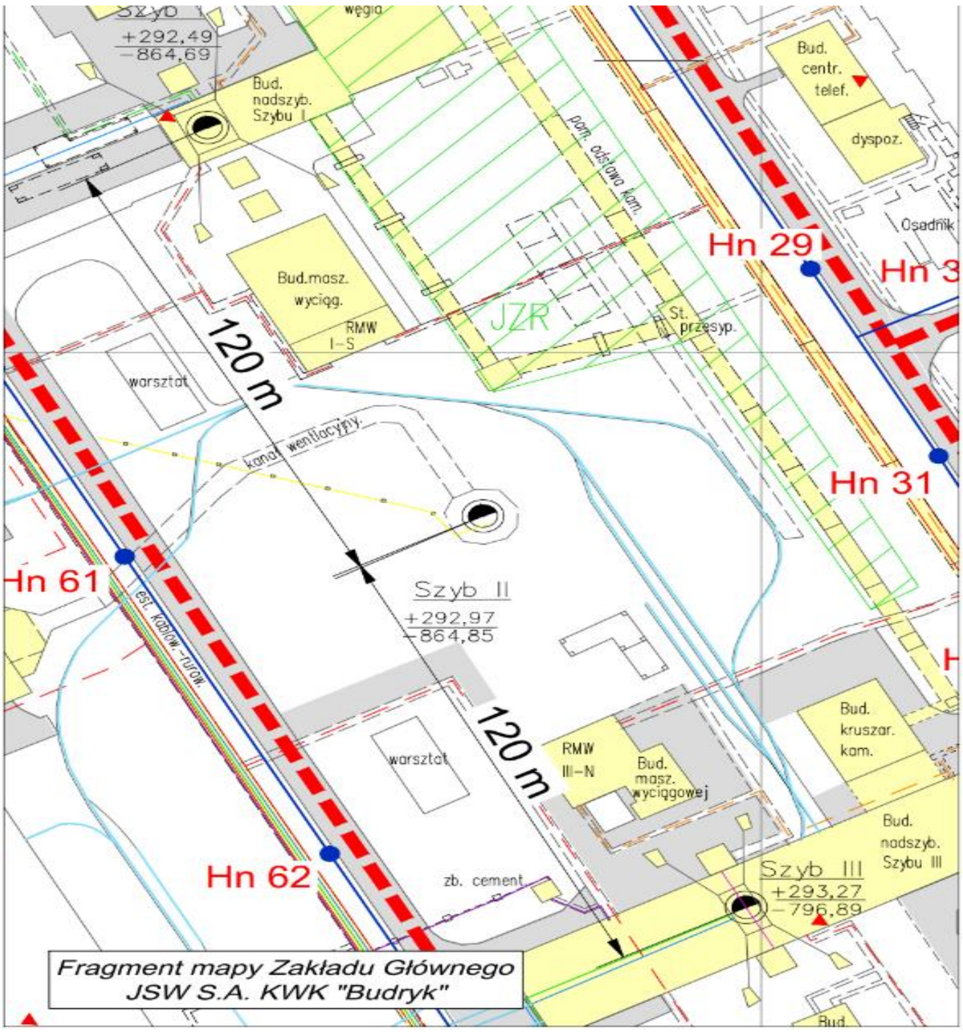

Figure 3 Maps of location Shafts I, II and III Budryk mine.

2. Geomechanical modelling of the shaft lining and its interaction with compressed air

The aim of this chapter is to verify the stability of the reference shaft lining under conditions of cyclic internal pressure resulting from the operation of the energy storage system. This analysis constitutes a key element of the definition of Baseline Conditions, allowing for the determination of safe operational limits for the existing engineering structure. The basis for the calculations is the assumption that the shaft is subjected to the action of compressed air with a maximum working pressure of 8 MPa. This value was adopted as the upper limit of the design envelope for CAES type reservoirs, although in operating conditions the system may work at lower pressure parameters, of the order of 5 or 6 MPa. Adopting the maximum value allows for the verification of the structure's behaviour in the most demanding load scenario.

2.1. Parameters accepted for analysis by the PRESS SHAFT application

The PRESS-SHAFT analytical tool, previously developed as part of this project, was used to perform the simulation. This application is based on a geomechanical model describing the stress and strain state in the shaft lining-rock mass system. The mathematical foundations of the model, including the utilized Coulomb-Mohr strength criterion and equations describing stress distribution in thick-walled pipes subjected to pressure, are consistent with the methodology adopted in previous stages of analytical works [2]. The use of dedicated software allowed for the generation of a stability profile for the entire shaft with a vertical resolution of 10 meters, which ensures significantly higher precision in detecting critical zones compared to standard sectional analyses.

The key stage in building the computational model was the introduction of input parameters that strictly reflect the technical and geological conditions of the Budryk III shaft. The material characteristics of the lining were defined based on the technical specification appropriate for the construction period of the facility, i.e., the 1980s. Analysis of archival documentation indicates that the shaft lining structure was made of class B30 concrete. According to contemporary classification standards, this corresponds to strength class C30/37. These parameters constitute a solid basis for calculations, considering that the long-term process of binder hydration in the mine environment favors the achievement of full design strength. In the analytical model, the lining structure was mapped as homogeneous, adopting strength parameters characteristic of this basic class of concrete. Omitting local reinforcement zones in the calculations, which according to documentation occur in seam opening areas, allows for the verification of structural stability in the most stressed variant, which constitutes a safe engineering margin. Tensile strength, which determines gas tightness, was determined directly based on the standard characteristics of the applied concrete class.

A complete description of the constitutive model of the lining material required defining the elastic constants that determine the stiffness of the structure and its susceptibility to deformation under cyclic pressure. Based on the standard physical properties of C30/37 class concrete, a static Young's modulus of 30 GPa was adopted. This parameter is of key importance for the analysis of the interaction between the lining and the rock mass, as it defines the ability of the concrete shaft pipe to transfer loads without excessive deformation. The transverse deformability characteristic was supplemented by adopting a Poisson's ratio of 0.2. This is a standard value for uncracked concrete, necessary for the correct calculation of stresses in the three-dimensional state of the geomechanical parameters of the surrounding environment were defined based on the detailed lithological profile of the Budryk III shaft. It was assumed that the type of rock in direct contact with the shaft lining is shale. This is the dominant formation in the geological profile of this specific shaft, while simultaneously being characterized by strength parameters constituting the lower limit for Carboniferous rocks occurring in this location. Such an approach eliminates the risk of overestimating the rock mass strength stiffness in areas where weaker layers occur.

The thermal load of the model is determined by local natural conditions and the technological specificity of the storage installation. The geothermal gradient was adopted in accordance with the thermal characteristics of the rock mass in the immediate vicinity of the shaft. The temperature of the working medium inside the shaft pipe was set at 50 degrees Celsius. This parameter results directly from the architecture of the CAES system integrated with the TES (Thermal Energy Storage) system. During the storage charging process, the air undergoes significant heating due to compression; however, before being injected into the shaft, it flows through the heat exchangers of the TES system. This system effectively extracts thermal energy, which is stored in a separate packed bed, and the medium entering the shaft is already cooled to a safe temperature. Thanks to this technological solution, the concrete lining is protected against thermal shock, and the temperature adopted in the calculations constitutes the upper, safe operational limit.

In order to fully replicate the material behaviour under a complex state, the strength characteristics were supplemented with a parameter describing the increase in concrete strength under triaxial compression conditions (rate of strength increase with the increase of the confining pressure). Based on the subject literature and the characteristics of structural concretes used in shaft construction, a coefficient value of 3.0 was adopted. This parameter allows for the inclusion of the beneficial effect of concrete confinement by the rock mass at great depths. Furthermore, the thermal model was calibrated by introducing a coefficient of linear thermal expansion for concrete at a standard level for crushed aggregates ($\alpha = 1{,}2 \bullet 10^{-5}$} K^{-1} as well as defining the boundary conditions of the temperature field. A value of 8°C was adopted as the reference temperature of the neutral zone at a depth of 10 meters b.g.l., corresponding to the multi-year average ground temperature in the Upper Silesia region.

Tab. 1 presents a summary of the input data implemented in the computational environment of the PRESS-SHAFT application.

Table 1 Input parameters for modelling in the PRESS-SHAFT application.

Parameter	**Unit**	**Value adopted for the model**
Shaft Lining Properties (Baseline)		
Concrete Class Reference	-	C30/37 (historical B30)
Unconfined Compressive Strength (UCS)	MPa	37.0
Tensile Strength	MPa	4.0
Young's Modulus	GPa	30.0
Poisson's Ratio	-	0.20
Rate of strength increase with the increase of the confining stress (pressure)	-	3.0
Internal Pressure in Energy Storage		
Maximum pressure of the medium	MPa	8.0
Thermal Properties		
Temp. of rock mass at -10 m bgl (reference)	°C	8.0
Temp. of medium inside the shaft (max)	°C	50.0
Thermal expansion coeff. of the shaft's lining	1/°C	0.000012
Temp. gradient of the rock mass	°C/m	0.03
Rock Mass Parameters (Clay Shale)		
Rock Mass Young's Modulus	GPa	5.7
Rock Mass Poisson's Ratio	-	0.24
Rock Mass Density	kg/m³	2650
Lining Thickness (baseline)	m	0.45

2.2. Simulation results and identification of critical areas

Based on the defined input parameters, a simulation of the lining stability for the full depth profile of the Budryk III shaft was conducted. The analysis of the results obtained using the PRESS-SHAFT application allows for the identification of characteristic zones of structural stress under a maximum working pressure of 8 MPa. The identified mechanisms of the structure's behavior are discussed in detail below, based on the generated calculation reports.

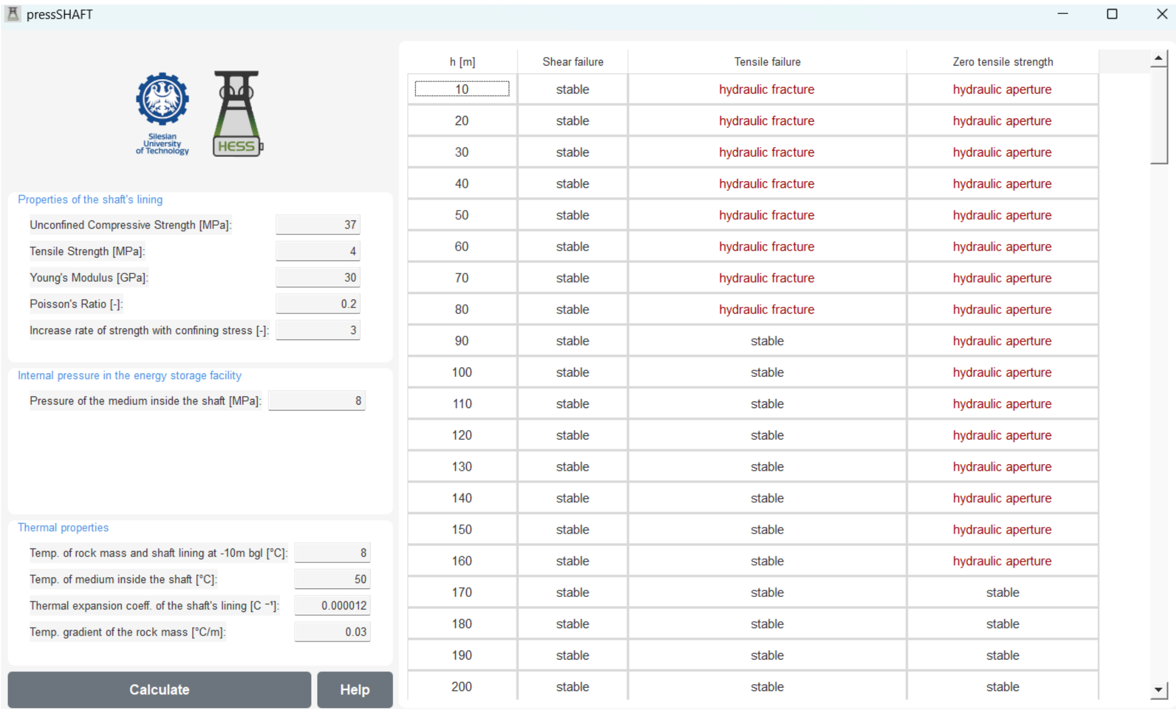

h [m]	Shear failure	Tensile failure	Zero tensile strength
10	stable	hydraulic fracture	hydraulic aperture
20	stable	hydraulic fracture	hydraulic aperture
30	stable	hydraulic fracture	hydraulic aperture
40	stable	hydraulic fracture	hydraulic aperture
50	stable	hydraulic fracture	hydraulic aperture
60	stable	hydraulic fracture	hydraulic aperture
70	stable	hydraulic fracture	hydraulic aperture
80	stable	hydraulic fracture	hydraulic aperture
90	stable	stable	hydraulic aperture
100	stable	stable	hydraulic aperture
110	stable	stable	hydraulic aperture
120	stable	stable	hydraulic aperture
130	stable	stable	hydraulic aperture
140	stable	stable	hydraulic aperture
150	stable	stable	hydraulic aperture
160	stable	stable	hydraulic aperture
170	stable	stable	stable
180	stable	stable	stable
190	stable	stable	stable
200	stable	stable	stable

Figure 4 Screenshot from the PRESS-SHAFT application presenting the results of the stability analysis for the upper section of the shaft.

The simulation results clearly indicate that for the adopted strength parameters of the concrete and at a maximum internal pressure of 8 MPa, there is no risk of lining failure due to shear (Shear failure). Throughout the analysed domain, from the collar to the shaft bottom, the structure maintains a stable status. This means that the resultant compressive stress state, resulting from the interaction between the rock mass pressure and the lining, does not exceed the ultimate compressive strength of the concrete, even when taking cyclic loading into account.

A key aspect of the analysis is the verification of the risk of lining cracking due to exceeding the tensile strength of the concrete (Tensile failure). The simulation revealed the existence of a potential hydraulic fracture risk zone in the near-surface section of the shaft, extending from the collar to a depth of 80 meters. This phenomenon results from the fact that at shallow depths, the rock mass pressure confining the lining is too low to compensate for the expansive action of the compressed air at 8 MPa. Only below the 90-meter level do the primary stresses in the rock mass, increasing with depth, effectively counterbalance the internal pressure, restoring the tensile stability of the lining.

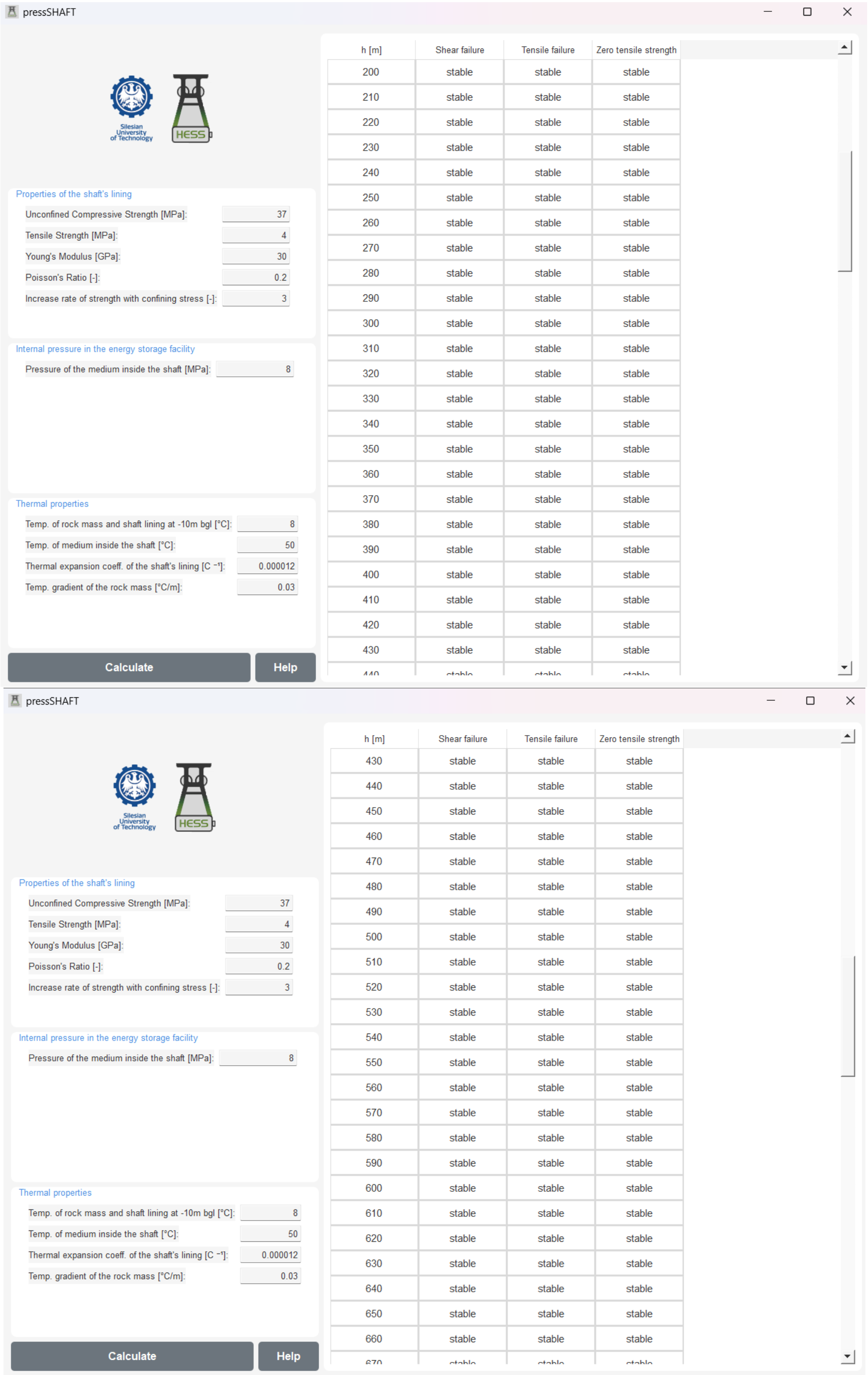

Figure 5 Screenshot from the PRESS-SHAFT application presenting the results of the stability analysis for section -200 to -660m.

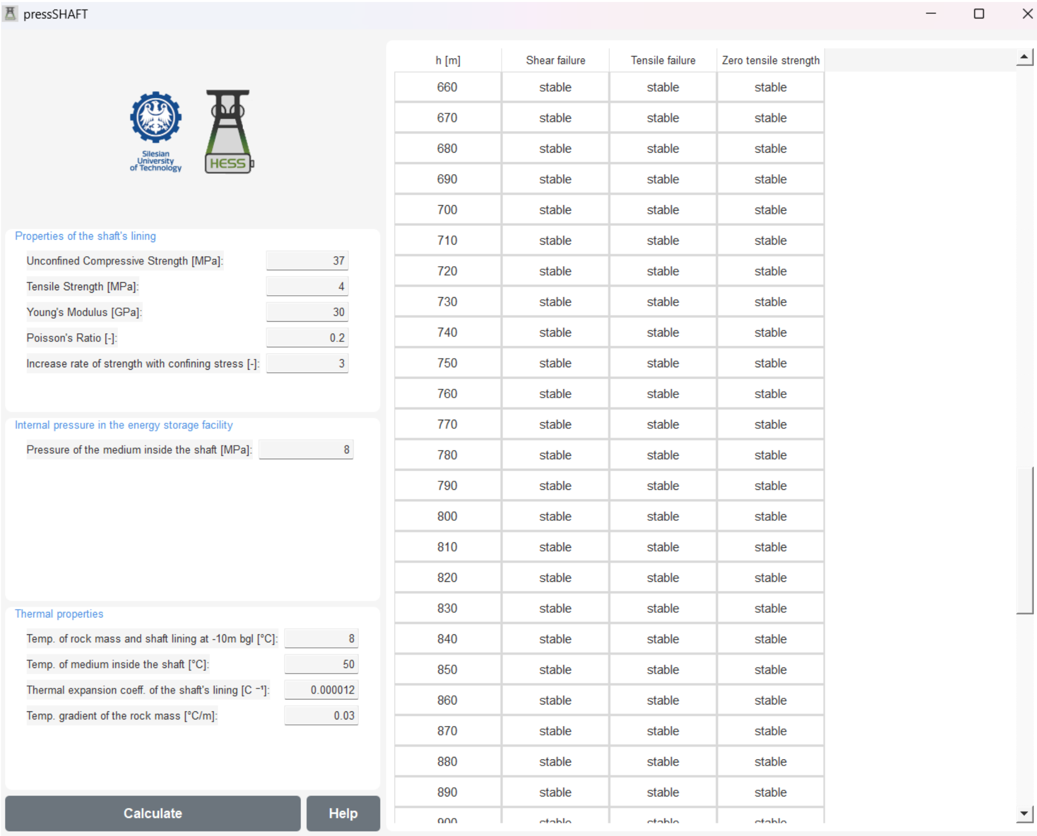

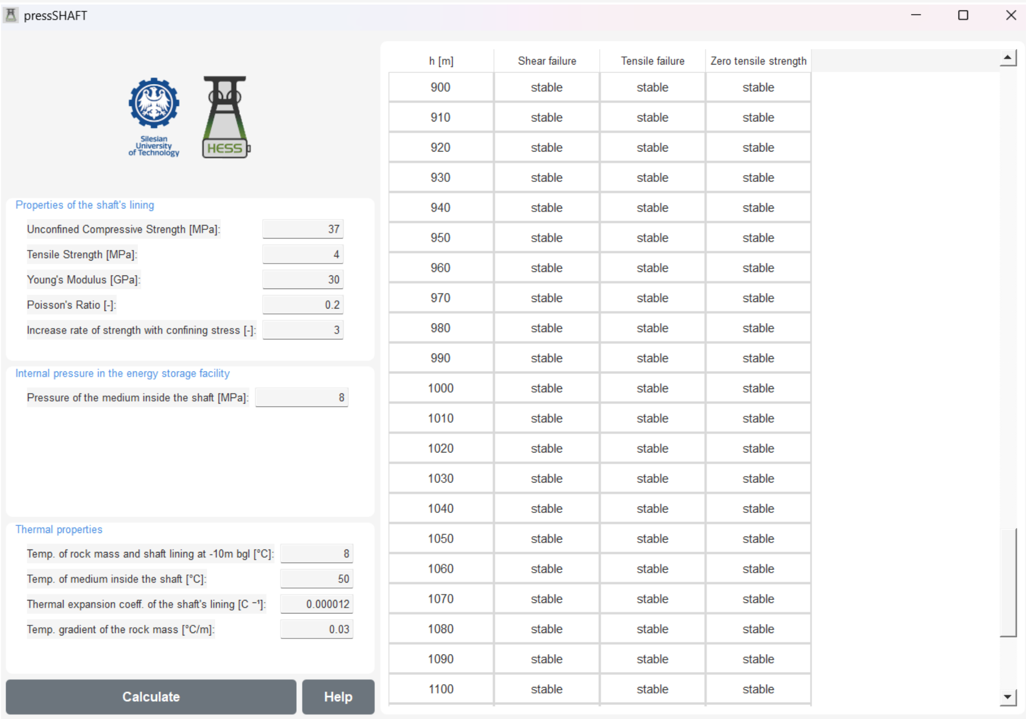

Figure 6 Screenshot from the PRESS-SHAFT application presenting the results of the stability analysis for section -670 to -11000m.

Simulation of lower section (Fig 5 and 6) show that lower part of shaft lining is stable.

2.3. Conclusions of the stability analysis in the context of shaft inlet protection

The conducted analytical analysis enabled the precise mapping of geomechanical risk zones. Although the results indicate a theoretical possibility of a loss of lining integrity in the zone up to 80 meters in depth, this threat is completely neutralized by the structural solutions adopted within the framework of the Baseline Conditions.

The adaptation concept for the Budryk III shaft, drawing directly on the technical solutions analysed in [3], assumes the construction of a massive reinforced concrete sealing plug, 100 m in length, in the upper section of the shaft (Fig. 7). Such geometry of the closing element ensures that the entire critical zone identified in the simulation, where the risk of tensile cracking occurred, is contained within the plug structure. This element, due to its construction and reinforcement, is designed as a self-supporting pressure vessel, capable of transferring the full load from the medium without the necessity of cooperation with the rock mass in terms of absorbing tensile forces. As a result, the negative impact of compressed air on the existing shaft lining in the zone of low primary stresses is physically eliminated, since the medium does not have direct contact with the primary lining in this section.

The working part of the reservoir, i.e., the space in which compressed air interacts directly with the existing shaft lining, begins below the 100-meter level, i.e., beneath the base of the plug. In this zone, the calculation results using the PRESS-SHAFT application unequivocally indicate a stable status. This means that throughout the entire active storage volume, the natural stress state in the rock mass is sufficiently high to effectively clamp the lining, counteracting the internal pressure. Thus, the adoption of a 100-meter-long plug constitutes sufficient technical protection, guaranteeing the full geomechanical stability of the facility under operational conditions.

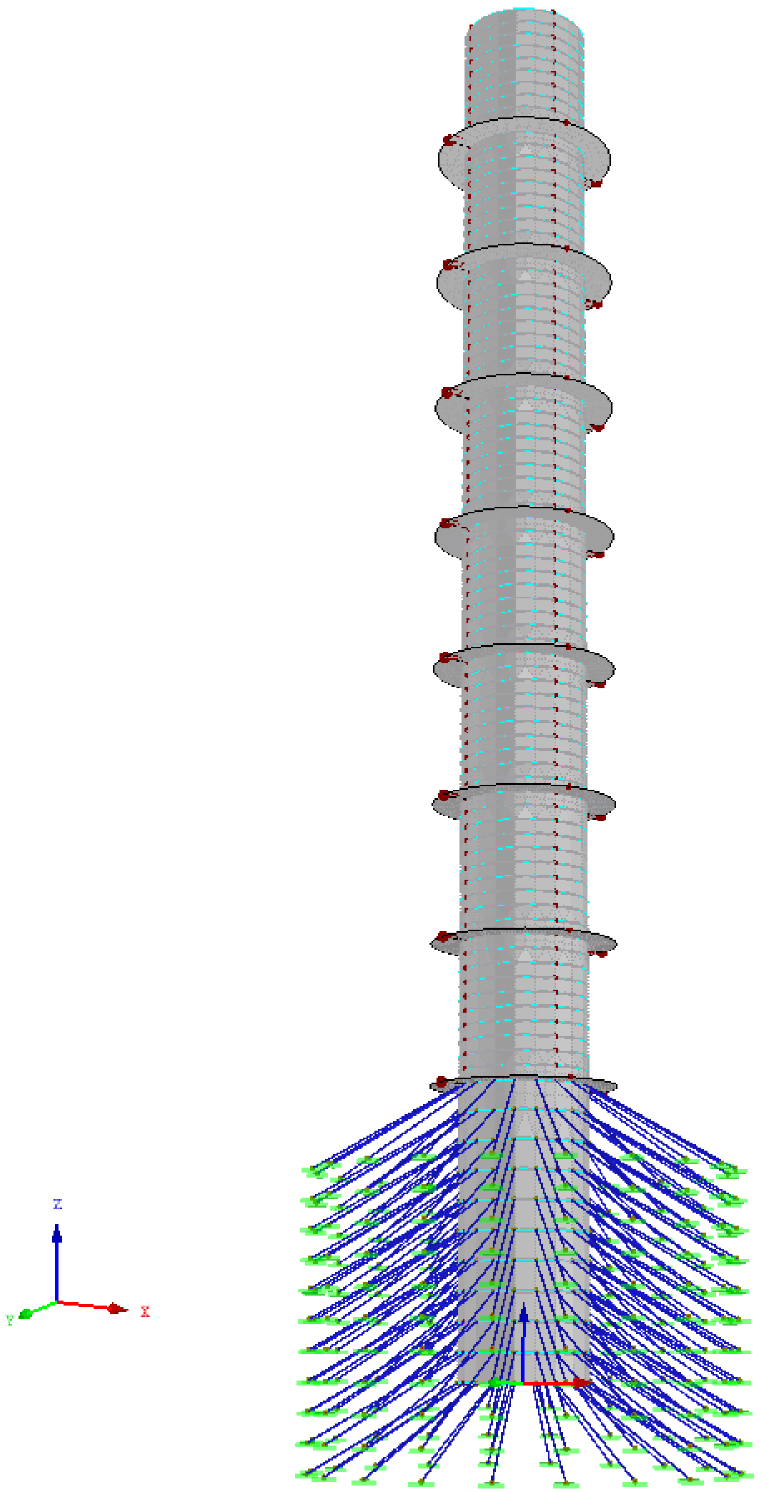

Figure 7 Simulation of a shaft plug showing the upper shaft section designed for sealing [3].

3. The impact of a fault or major fracture in the rock mass on the stability of a circular shaft and the safety of use of the energy storage facility located therein

The selection of one of the shafts in the Budryk colliery – Shaft III – means that, to design its use as an energy storage facility, it is necessary to check from a geomechanical point of view whether there is a fault zone in its immediate vicinity. The Budryk mine is a prime example of a shaft being intersected by a fault and the problems associated with this. In Shaft VI, located relatively close to Shaft III, at only about 3.5 km, during the deepening of this shaft from a depth of 1,034 m achieved during the construction of the mine to 1,320 m, it was discovered that a fault (the so-called Chudecki fault) runs through the shaft at a depth of approximately 1,170 - 1,230 m. This fault causes great difficulties in maintaining the stability of Shaft VI and the station at a level of -1290 m.

Therefore, before constructing an energy storage facility, e.g. in Shaft III of the Budryk mine or any other mine, it is necessary to check whether there is a fault zone in close proximity to the shaft that could be activated by using the shaft as an energy storage facility. If such a fault is found, the analysis described in the subchapter below can be used for a preliminary assessment of the hazard involved. The course of the fault, its distance from the shaft and its orientation in relation to the directions of horizontal stresses will be of greatest importance here. In many cases, there will be no need to conduct costly, complex and time-consuming analyses, and if so, it will be to confirm the validity of their commissioning (execution) for the investor.

An analysis has been conducted to address the fundamental question in rock and strata mechanics: how valid are the estimates obtained for the elastic stress distribution around a circular shaft when the boundary of an opening is intersected by a plane of weakness?

Five, the most frequently found orientations of the plane of weakness have been analyzed and it has been assumed that the discontinuity has zero value for tensile strength and cohesion and is non-dilatant in shear, so it is a crack in nature.

As a result, it has been concluded that, in some cases, planes of weakness may have little or no effect on the boundary stresses. In cases where the boundary stresses are affected by the rock structure, the most important factors contributing to alteration of the elastic stresses have been found to be the orientation of the joint, joint shear strength and/or far field stress state in a rock mass.

3.1. Fundamentals of Stress Analysis Around Circular Excavations

In rock mechanics, the formulas provided by Kirsch [10] for describing the stress and displacement conditions in the vicinity of a circular cross-section opening are probably the most used set of equations from elasticity theory (see, for example, [8,9]). They are used to determine the stability of circular cross-section tunnels or shafts, but also in methods of measuring stresses in rocks and, for example, in hydraulic fracturing used to intensify the extraction of gas or oil from both conventional and unconventional deposits. These equations, which allow for the analysis of the stress state in a medium subjected to stresses, such as those in rock masses, are particularly useful in geoengineering, but their validity applies only to continuous, isotropic media that behave in a perfectly linear-elastic manner.

In view of the above, the question arises: to what extent do the conclusions from their application retain their value when the shaft is intersected by a fault or major crack or a plane of weakness runs in its immediate vicinity?

As part of this task, the project undertook to determine under what conditions the conclusions from the classical analysis of the impact of a circular cross-section shaft in a rock mass with the characteristics of an ideally linear-elastic medium on the stress state in its surroundings remain valid when the excavation is crossed by or runs close to a single main discontinuity.

The analysis allows for the establishment of certain practical guidelines indicating the conditions under which the plane of weakness has little effect on the stress and displacement conditions in the vicinity of the shaft. It also allows, with the help of relatively simple conceptual models, for an engineering assessment of the impact of individual parameters on the stability of the excavation when the impact of discontinuities is significant.

The stability of the shaft as an energy storage facility and the long-term safety of its use will be significantly affected by the stress conditions around the shaft, and more specifically by the horizontal stresses around it. The more heterogeneous the stress state, especially the greater the difference between horizontal stresses, the greater the risk of shaft instability, especially through the activation of geological discontinuities (fractures, faults) and slippage along their course. It is crucial to know the values and directions of horizontal stresses around the shaft, as the cycles of compression and expansion of compressed air or the increase in pressure inside the shaft associated with the presence of water in the case of pumped storage power plants can lead to the activation of discontinuities running directly through the shaft or located in its immediate vicinity, which remain inactive under normal mining conditions.

Due to the circular shape of the shaft, for the sake of precision of the information provided in this chapter, we will use the terms north-south (N-S) and east-west (E-W) horizontal stresses, and interchangeably - the direction of the major principal stress and the direction of the minor principal stress. I assume that the major principal stress, which I also assume to be one of the horizontal stresses, will act in the north-south (N-S) direction, and the minor principal stress, which is also a horizontal stress, will act in the east-west (E-W) direction. The symmetry of the problem means that, whenever the principal stresses are not oriented in the N-S and E-W directions, the conclusions of this analysis are still true but there is just a need for adjustment by rotation. They will also remain valid if it turns out that the vertical stress is not an intermediate principal stress, but either the major or minor principal stress. This does not affect the correctness of the analysis or the relevance of its conclusions.

3.2. Analysis of the impact of the weakness plane on the stress and displacement state in the rock mass surrounding the shaft.

Five of the most typical cases of mutual orientation of discontinuities relative to the shaft were analysed, collected and presented schematically in Table 2, with the discontinuity defined as having zero cohesion and tensile strength. It was also assumed that the discontinuity has high stiffness in both the normal and tangential directions, so that the effect of the elastic deformation of the discontinuity itself on the change in stress in the rock mass is negligible, and that there is no dilational opening of the discontinuity when its walls move relative to each other. The shear strength of the discontinuity is given by the classic relationship:

$$\tau = \sigma_n \operatorname{tg} \phi \qquad (1)$$

where:

τ – shear strength of the discontinuity, MPa;

σ_n – normal stress in the discontinuity plane, MPa;

ϕ – friction angle, °.

a) Discontinuity passing through the shaft axis oriented along the direction of the minor principal stress (horizontal)

Tangential stresses along the horizontal axis of the excavation (φ=0) take values equal to 0 for any r (see formulas 2-7). The shear stresses acting along the horizontally oriented plane of weakness passing through the axis of the excavation therefore also take the value zero and there is no slip along the discontinuity (Fig. 8).

– radial stress σ_r:

$$\sigma_r = \frac{\sigma_z}{2}\left[1 - \frac{a^2}{r^2} - \left(1 - 4\frac{a^2}{r^2} + 3\frac{a^4}{r^4}\right) cos2\varphi\right] + \frac{\sigma_x}{2}\left[1 - \frac{a^2}{r^2} + \left(1 - 4\frac{a^2}{r^2} + 3\frac{a^4}{r^4}\right) cos2\varphi\right] \qquad (2)$$

lub

$$\sigma_r = \frac{\sigma_z}{2}\left[(1+k)\left(1 - \frac{a^2}{r^2}\right) - (1-k)\left(1 - 4\frac{a^2}{r^2} + 3\frac{a^4}{r^4}\right) cos2\varphi\right] \qquad (3)$$

– tangential (circumferential) stress σ_φ:

$$\sigma_\varphi = \frac{\sigma_z}{2}\left[1 + \frac{a^2}{r^2} + \left(1 + 3\frac{a^4}{r^4}\right) cos2\varphi\right] + \frac{\sigma_x}{2}\left[1 + \frac{a^2}{r^2} - \left(1 + 3\frac{a^4}{r^4}\right) cos2\varphi\right] \qquad (4)$$

$$\text{lub } \sigma_\varphi = \frac{\sigma_z}{2}\left[(1+\mathrm{k})\left(1 + \frac{\mathrm{a}^2}{\mathrm{r}^2}\right) + (1-\mathrm{k})\left(1 + 3\frac{\mathrm{a}^4}{\mathrm{r}^4}\right)\cos 2\varphi\right] \qquad (5)$$

– shear stress $\tau_{r\varphi} = \tau_{\varphi r}$:

$$\tau_{r\varphi} = \tau_{\varphi r} = \frac{\sigma_z - \sigma_x}{2}\left(1 + 2\frac{a^2}{r^2} - 3\frac{a^4}{r^4}\right) sin2\varphi$$
(6)

lub $$\tau_{r\varphi} = \tau_{\varphi r} = \frac{\sigma_z}{2}\left[(1-k)\left(1 + 2\frac{a^2}{r^2} - 3\frac{a^4}{r^4}\right) sin2\varphi\right]$$
(7)

Table 2 Variants of discontinuity location relative to the shaft.

1	2
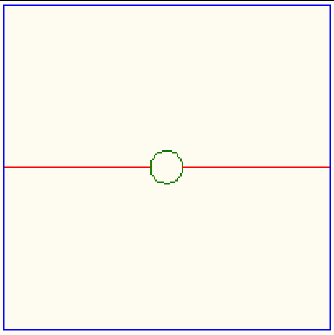	Case I – discontinuity passing through the shaft axis oriented along the direction of the minor principal stress (horizontal)
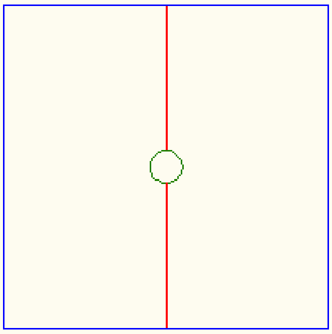	Case II – discontinuity passing through the shaft axis oriented along the direction of the major principal stress (horizontal)
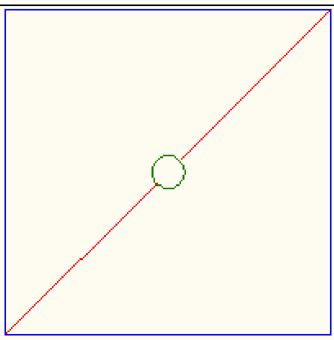	Case III – discontinuity passing diagonally through the shaft axis
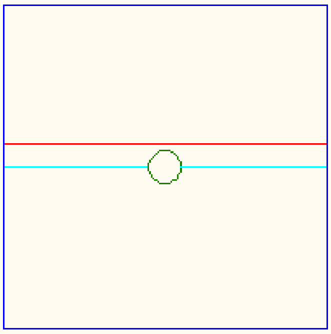	Case IV – discontinuity located in close proximity to the shaft, running parallel to the direction of the minor principal stress (horizontal)

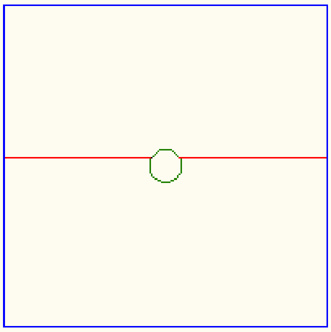	Case V – discontinuity crossing the shaft, running parallel to the direction of the minor principal stress (horizontal)

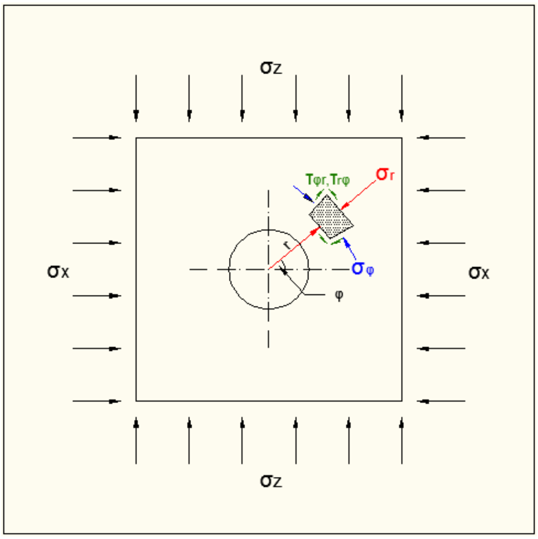

Figure 8 State of stress around a circular cross-section shaft (where σ_x i σ_z – horizontal components, W-E and N-S, respectively, of the stress state acting in the rock mass at a large distance from the excavation; r i φ - polar coordinates; σ_r – radial stress; σ_φ – circumferential stress; $\tau_{\varphi r} = \tau_{r\varphi}$ – shear stresses).

In this case, the location of the shaft relative to the plane of weakness does not affect the stress state around the excavation, and the conclusions from the classical analysis based on Kirsch's solution remain valid.

b) Discontinuity passing through the shaft axis oriented along the direction of the major principal stress (horizontal)

For an angle $\varphi=\pi/2$, no shear stresses will be generated along the discontinuity – thus, there is no tendency for slippage along the discontinuity, and the stress state around the shaft is not modified by the shear displacement of the discontinuity walls. However, it is known that the discontinuity walls may open if tensile stresses occur. From Kirsch's equations, it is known that this will occur when the ratio of primary stresses in the W-E direction to those in the N-S direction is less than 1/3 (k<1/3).

In this case, the opening of the discontinuity along the N-S direction leads to the formation of stress relief zones. The size of the stress-relieved zone can be estimated for design purposes by assuming that it can be compared to an ellipse, one axis of which is identical to the diameter of the excavation oriented along the W-E direction, and the length of the other semi-axis is determined by the maximum range of tensile stresses along the N-S direction. The walls of the discontinuity do not open up when the magnitude of normal stresses is zero, so as a consequence, the condition arises that the magnitude of horizontal stresses in the W-E direction at the apex of the ellipse is zero:

$$\sigma_B = \sigma_x \cdot \left(1 + 2\frac{H}{W}\right) - \sigma_z = 0 \qquad (8)$$

and

$$H = 2a + 2\Delta h \qquad (9)$$

and in addition

$$W = 2a \qquad (10)$$

which leads to a relationship allowing the range of the relaxed zone along the N-S direction to be determined:

$$\Delta h = a\left(\frac{1-3k}{2k}\right) \qquad (11)$$

where:

σ_B – circumferential stress at the apex of the ellipse, in the N-S direction, MPa;

Δh - extent of the relaxed zone along the N-S direction, m;

a – shaft radius, m;

k - coefficient of proportionality between the values of horizontal stresses W-E and N-S;

H – axis of the ellipse in the N-S direction, m;

W - axis of the ellipse in the W-E direction, m;

c) discontinuity passing diagonally through the shaft axis

When the discontinuity passes through the shaft axis, intersecting it at an acute angle (the symmetry of the problem allows the conclusions to be easily extended to the case where the angle becomes obtuse), the circumferential stresses are normal stresses to the discontinuity, and the shear stresses attempting to induce shearing along the discontinuity are expressed by the formulas (6) or (7). The ratio of shear stresses to normal stresses, in accordance with the assumed failure criterion (1) determining the shear strength of the discontinuity, allows the value of the external friction angle to be determined for which slippage along the fracture will occur. For example, for a stress state (e.g. primary) in which the horizontal stresses in the W-E direction are half of the horizontal stresses acting in the N-S direction and the angle of inclination of the discontinuity is 45°, formulas (5) and (7) take the form:

d) $\sigma_n = \sigma_\varphi = \frac{3\sigma_z}{4}\left(1 + \frac{a^2}{r^2}\right)$ (12)

e)

f) $\tau = \tau_{r\varphi} = \tau_{\varphi r} = \frac{\sigma_z}{4}\left(1 + 2\frac{a^2}{r^2} - 3\frac{a^4}{r^4}\right)$ (13)

g)

Figure 9 shows the relationship between the change in the value of the τ/σ_n ratio and the distance from the shaft contour given by the ratio of the radius (polar coordinate) to the shaft radius. An additional ordinate axis has been added to indicate the friction angle values corresponding to the given values of the ratio of shear to normal stresses.

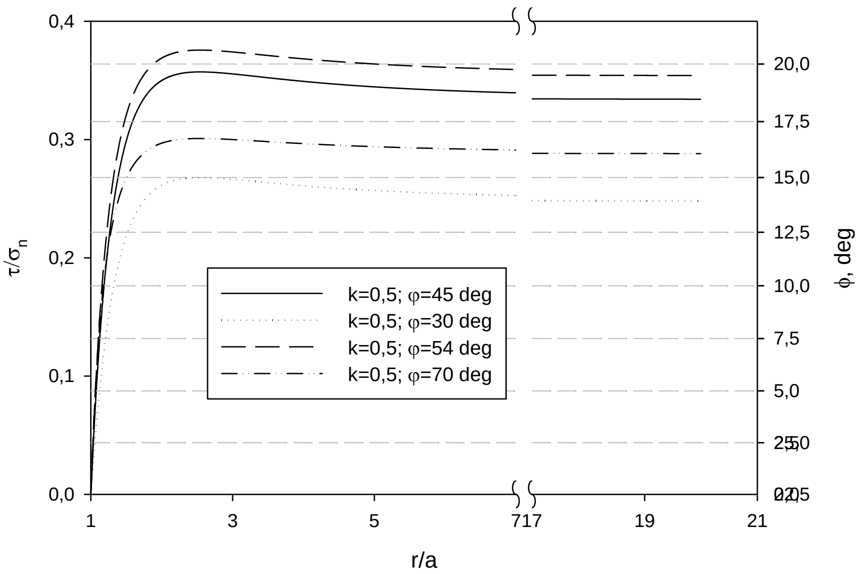

Figure 9. The dependence of the τ/σ_n ratio on the normalized distance from the shaft contour for discontinuities intersecting the shaft at example acute angles, when the primary horizontal stresses in the W-E direction are half of the horizontal stresses in the in the W-E direction are half of the horizontal stresses in the N-S direction, and the shaft radius is 2.5 m.

For an excavation with a radius of 2.5 m, the maximum value of τ/σ_n equal to approximately 0.357 occurs for r/a slightly above 2.5 (2.54) and corresponds to a friction angle of approximately 19.65°. As the distance from the shaft increases, the value of the angle ϕ decreases slightly, asymptotically approaching approximately 18.43° ($\tan^{-1}(1/3)$).

This means that if the rock mass is in a state of limit equilibrium (ϕ ≈18.5°), increasing the pressure of the working medium in the shaft energy storage facility (e.g. compressed air or water) may cause shear displacement of a large part of the rock mass due to slippage along the discontinuity. On the other hand, if the friction angle of the discontinuity exceeds 19.6°, no slip will occur along any part of it.

At other angles of inclination of the discontinuity passing through the shaft, the friction angle required to prevent slippage changes. For example, a decrease in the angle of inclination of the discontinuity means that discontinuities with lower shear strength do not slip as easily; for an angle of inclination of 30°, no slippage will occur at all if the friction angle is approximately 15° and approximately 13.9° at a greater distance from the shaft.

Increasing the angle of inclination of the discontinuity results in a change in the required angle of friction. For an angle of 54°, which characterises the most unfavourable inclination for this stress state (k=0.5) , the friction angle guaranteeing no slippage should be at least approximately 20.6°, and in order for slippage not to occur at a greater distance from the shaft, the required value of the angle ϕ increases to approximately 19.5°.

In general, increasing the slope above 45° results in an increase in the required friction angle necessary to prevent significant shear displacement along the fracture. However, depending on the stress state, the relationship $\tau/\sigma_n = f(\varphi)$ reaches its maximum at different values of the discontinuity slope angle (Fig. 3). For example, for an inclination angle of 70°, no slippage will occur if the friction angle is only 16.75°, and at a greater distance from the shaft, approximately 16° (see Fig. 9).

The values of the angle of inclination of the discontinuity at which the highest shear strength (expressed by the angle of friction) is necessary to prevent slippage increase the more asymmetrical the stress state is. At a point located along the discontinuity, two and a half times the radius away from the centre of the excavation, for horizontal stresses in the W-E direction constituting 75% of the horizontal stresses in the N-S direction, the maximum occurs for an angle of inclination of approximately 49°. When the horizontal W-E stresses decrease in relation to those acting in the N-S direction, the values of the angle of inclination at which extreme values of the τ/σ_n increase: for k=½ they occur at φ=54°, when $\sigma_x = ¼\sigma_z$ for φ=62°, and when k=0.11 even at almost 70° (69°) (see Fig. 10).

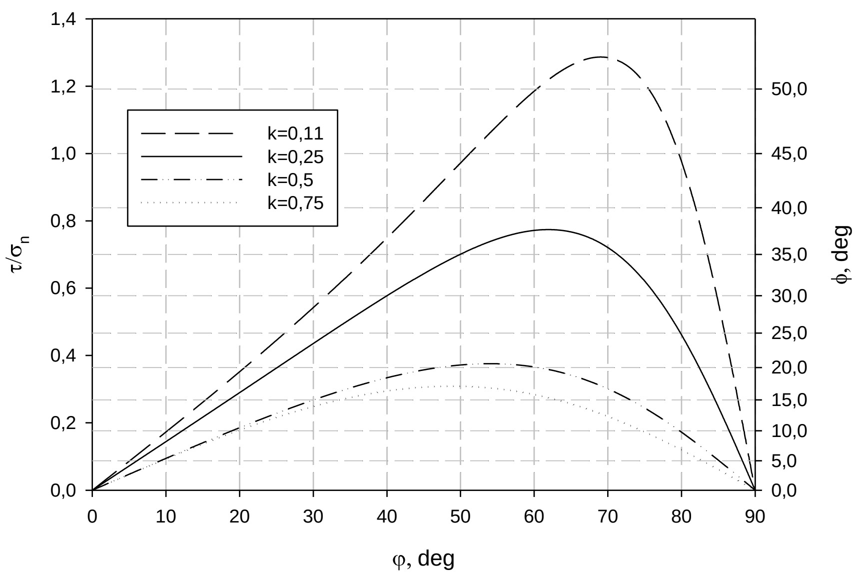

Figure 10 The relationship between the value of the τ/σ_n corresponding to the friction angle and the angle of inclination of the discontinuities intersecting the shafts, with a variable ratio of primary horizontal stresses in the W-E direction relative to those in the N-S direction, for r/a=2.5.

The influence of the stress state in the rock mass on the occurrence of slip along the entire surface of the discontinuity is illustrated in Figure 11.

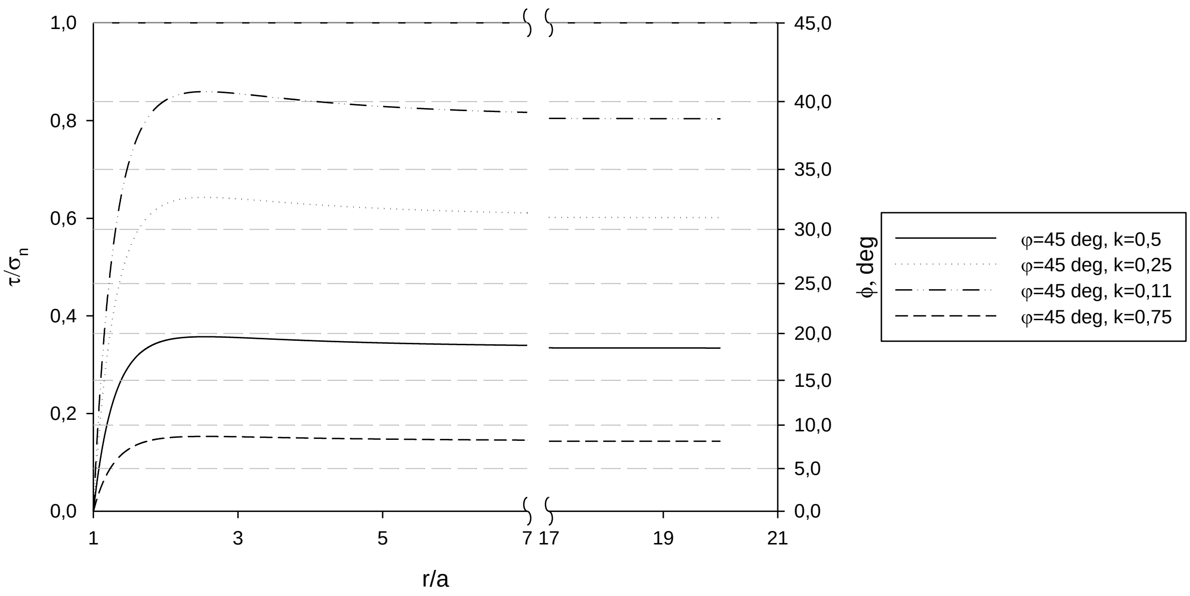

Figure 11The dependence of the τ/σ_n ratio on the normalised distance from the shaft for discontinuities intersecting the shaft at angles of 45°, with a variable ratio of primary horizontal stresses in the W-E direction to those in the N-S direction.

For example, for a discontinuity inclined at an angle of 45°, a more asymmetrical stress state results in an increase in the friction angle required to prevent slippage. For $\sigma_x=\frac{1}{4}\sigma_z$, the friction angle guaranteeing no slippage should be at least approximately 32.75°, and in order for slippage not to occur at a greater distance from the excavation, the required value of the angle ϕ increases to approximately 32° (31.03°). When the horizontal stresses in the W-E direction are approximately 11% of the horizontal stresses in the N-S direction, the values of both angles reach over 40.5° (40.675°) and 38.79°, respectively. A more homogeneous stress state, in turn, means that in order to prevent slippage along the discontinuity, a much lower shear strength is required. When $\sigma_x=\frac{3}{4}\sigma_z$, the friction angle indicating no slippage can be even less than 9° (8.6°). In order for slippage not to occur at a greater distance from the excavation, it should be slightly more than 8° (8.15°).

d) A discontinuity located in close proximity to the shaft, running parallel to the direction of the minor principal stress (horizontal)

Using the transformation equations for the stress state and the equations from Kirsch's solution, the normal and shear stresses acting in the plane of discontinuity can be easily determined. Assuming, for example, that the rock mass is in a hydrostatic stress state ($\sigma_x=\sigma_y=\sigma_z$), these equations take the following form:

$$\sigma_n = \sigma_z \left(1 - \frac{a^2}{r^2}\cos 2\varphi\right) \tag{14}$$

$$\tau = \sigma_z \frac{a^2}{r^2}\sin 2\varphi \tag{15}$$

The values of τ/σ_n ratio determined from the above equations are shown for points along the discontinuity, for several example radii of the shaft, assuming that the distance between the fracture running along the direction of the minor principal stress and the shaft is constant and equal to c=1 m (Fig. 5).

For an excavation with a radius of 1.25 m, a friction angle of 15° is sufficient to prevent shear displacement along the discontinuity. Increasing the radius to 2.5 m means that at an angle of friction of 15°, slippage will occur over a distance of more than 3.5 m, from a point located approx. 0.45 m above the shaft axis to a point almost 4 m away (see Fig. 12). The required friction angle to prevent slippage increases to almost 28° (27.83°). Increasing the shaft diameter results in even higher maximum values of τ/σ_n ratio. For a radius of 3.5 m, this value is already 0.704 (ϕ = 35.17°) and for a shaft with a radius of 5 m, it is even around 0.926 (ϕ = 42.79°).

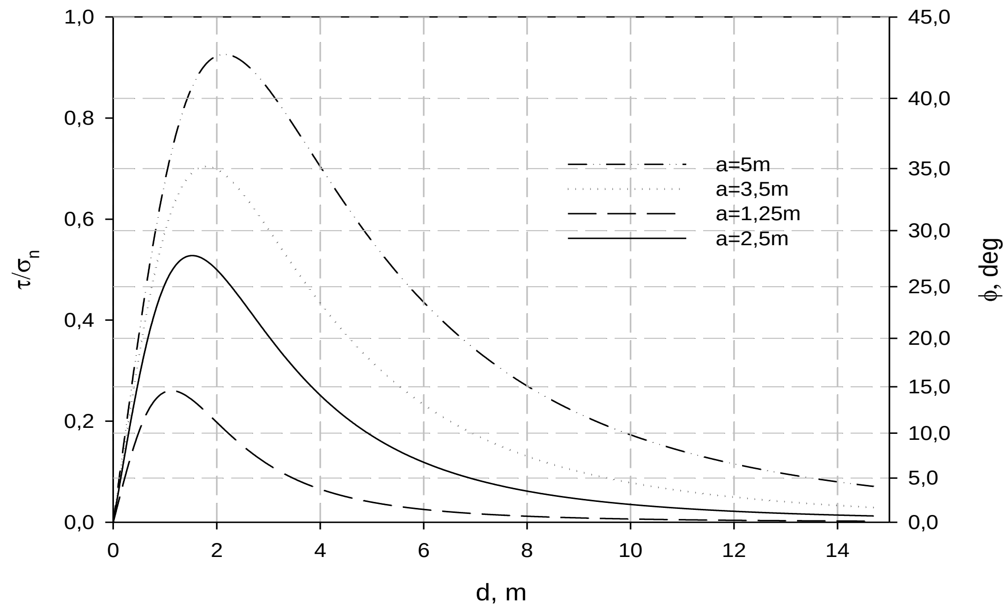

Figure 12 The dependence of the value of the ratio τ/σ_n along the discontinuity, starting from a point above the shaft axis, for different values of the shaft radii – a, when the fracture runs along the direction of the minor principal stress, at a distance of 1 m from shaft.

The slip will also occur symmetrically on the other side of the shaft axis. For both zones, the nature of the shear displacement will be such that the upper part of the discontinuity (the part on the outer side of the discontinuity, further away from the shaft) will move outwards from the shaft in relation to the lower surface. This will cause stress concentration in the rocks between the shaft and the fracture.

For a given shaft diameter, the distance at which the fracture runs from the shaft has an incredibly significant impact on the possibility of slip occurring along the discontinuity located in its vicinity (Fig. 13).

For example, when the shaft radius is 2.5 m, even a slight change in the distance between the shaft and the fracture results in a dramatic change in the maximum values of the τ/σ_n ratio. When the shaft is 0.5 m away from the fracture, $(\tau/\sigma_n)_{max}$ is greater than 1, and the corresponding friction angle exceeds 45°.

Moving the shaft 2 m away from the crack causes the friction angle required to prevent slippage to drop below 15° (14.19°).

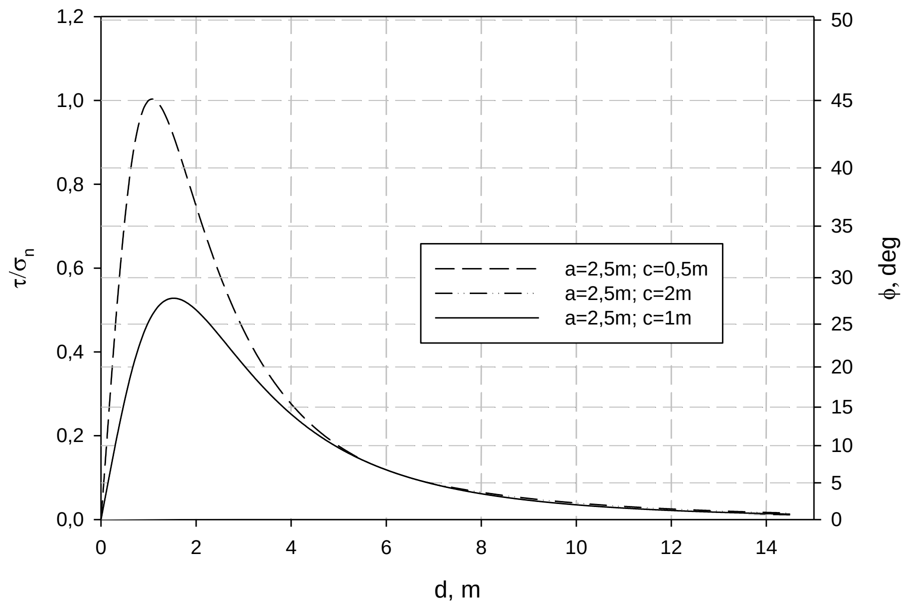

Figure 13 The dependence of the value of the ratio τ/σ_n along the discontinuity, starting from a point lying above the shaft axis with a radius of 2.5 m, when the fracture runs along the direction of the minor principal stress, at various distances from the shaft.

e) discontinuity crossing the shaft, running parallel to the direction of the minor principal stress (horizontal)

The normal and shear components of the stresses acting in the plane of discontinuity are:

$$\sigma_n = \sigma_\varphi(\cos\varphi)^2 \qquad (16)$$

$$\tau = \sigma_\varphi \sin\varphi \cos\varphi \qquad (17)$$

Taking into account the failure criterion defining the shear strength of a discontinuity given by formula (1), we obtain:

$$\sigma_{\varphi} \sin\varphi \cos\varphi = \sigma_{\varphi} (\cos\varphi)^2 \operatorname{tg}\phi \quad (18)$$

and after conversion:

$$\operatorname{tg}\varphi = \operatorname{tg}\phi \quad (19)$$

In the case of a discontinuity running parallel to the direction of the minor principal stress, passing through the excavation not in its axis but at a certain distance from it, the possibility of slippage is determined precisely by this distance from the shaft axis. At a given shear strength of the discontinuity, slippage will occur when the angle of inclination of the radius (polar coordinate) connecting the centre of the shaft and the beginning of the discontinuity on its circumference is greater than the angle of friction of the discontinuity.

The nature of the shear displacement will be such that the upper part of the discontinuity (the part on the outer side of the discontinuity, further from the shaft axis) will move outwards from the shaft in relation to the lower surface. This will reduce the stress in the rocks located directly behind the shaft lining on the outer side of the fracture, further from the shaft axis. It is therefore possible for fissures, which are quasi-perpendicular to the main fracture, to form there, in the immediate proximity of the shaft [5].

If the excavation is located in a layered rock mass, so that it is traversed not by a single discontinuity but by a set of parallel fractures oriented parallel to the direction of the minor principal stress, slippage will occur along each of the discontinuities for which the condition ($\varphi > \phi$) is satisfied [4].

3.3. Evaluation of Stress and Deformation Around Circular Shafts

The task involved determining the conditions under which the conclusions from the classical analysis of the impact of sinking a circular cross-section shaft on the state of stress in its vicinity, in a rock mass with the characteristics of an ideally linear-elastic medium, remain valid when the shaft intersects or is located in close proximity to a major discontinuity, such as a fault or fracture.

Five typical cases of the most representative locations of the discontinuity relative to the shaft were analysed, with the discontinuity characterised by zero cohesion and tensile strength.

The presented method of analysis allows to determine under what conditions inelastic shear displacements and/or opening of discontinuities may occur in the vicinity of the shaft and whether they should be the subject of detailed study by engineers designing energy storage facility in the shaft. When the analysis shows that the magnitude of inelastic deformations caused by the discontinuity is insignificant, the effect of the discontinuity on the state of stress and displacement around the shaft can be neglected and a classical analysis using Kirsch's solution can be performed. When the inelastic effects are significant and their impact is not negligible, numerical analyses are highly desirable. In this case, the results of the simple analyses presented in this chapter provide valuable information. They allow for a quick and inexpensive analysis of the impact of many parameters taken into account in the design process, such as: the location of the shaft, its size (diameter), orientation in relation to the stress state in the rock mass, its stability, ease of maintenance and safety of use of the energy storage facility. Both the creators of the best numerical modelling tools and prominent consultants and researchers recommend conducting such simple analyses before proceeding to more advanced studies (see for example [5, 6, 7]).

As part of the task, after performing the analyses presented above, numerical models of the rock mass and a circular cross-section shaft were constructed, and numerical simulations were carried out. The numerical analyses performed using the discrete element method confirmed the conclusions of the analytical work and enabled a more complete analysis and description of the state of stress, deformation, displacement and strain around a circular shaft in a rock mass with a single main fracture.

The method of conducting numerical analyses and their results is presented in a separate deliverable [2].

4. Summary and conclusion

This deliverable establishes the Baseline Conditions for the reference shaft selected within the HESS project, defining the minimum acceptable technical, structural, and geomechanical state required for the safe adaptation of an existing mine shaft into a high-pressure compressed air energy storage facility. The Budryk III shaft was adopted as the reference object based on a multi-criteria decision analysis performed in earlier project stages, ensuring that the guidelines are grounded in a representative and technically robust case study. The document integrates the results of previous work packages by translating the outcomes of the MCDA-based preselection (WP2) and advanced geomechanical modelling using the PRESS-SHAFT application (WP3) into a coherent set of engineering guidelines. These guidelines define admissible ranges of geometric parameters, lining properties, rock mass characteristics, and hydrogeological conditions that collectively determine the suitability of a shaft for pressurised operation. Detailed numerical analyses confirmed that, under the assumed maximum internal pressure of 8 MPa, the existing shaft lining remains stable over the entire active storage depth, with the exception of the shallow near-surface zone where tensile cracking may theoretically occur. This risk is effectively mitigated by the adoption of a 100-m-long reinforced concrete sealing plug, which isolates the critical zone and ensures that the compressed air interacts only with shaft sections where the surrounding rock mass provides sufficient confinement. Additional analytical and numerical investigations addressed the potential impact of geological discontinuities, demonstrating under which stress and structural conditions faults or fractures may influence shaft stability. The results provide practical criteria for assessing when simplified analytical approaches are sufficient and when more advanced numerical modelling is required.

Overall, Deliverable D4.2 provides a validation framework for assessing existing mine shafts against clearly defined baseline requirements. These guidelines constitute a necessary technical reference for subsequent design, material testing, and adaptation activities within WP4, ensuring consistency between theoretical models, safety considerations, and the actual condition of post-mining infrastructure considered for energy storage applications.

5. Literature

[1] Deliverable 2.1 of HESS project, Guidelines on the adaptation and use of inactive shafts possible to energy storage, 30.06.2024, D. Kowol, P. Matusiak, D. Czerniak, D. Bałaga, M. Lutyński, K. Kołodziej, Ł. Bartela, K. Labus, G. Smolnik, J. Ochmann, A. Niewiadomski, https://itpe.pl/wp-content/uploads/2024/11/D.2.1_HESS_Guidelines-on-the-adaptation-and-use-of-inactive-shafts-possible-to-energy-storage.pdf

[2] Deliverable 3.2. of HESS project, Technical parameters of the example underground water reservoir model, G. Smolnik, K. Kołodziej, A. Niewiadomski, M. Lutyński, 31.12.2024, https://itpe.pl/wp-content/uploads/2025/03/D.3.2_HESS_Technical-parameters-of-the-example-underground-water-reservoir-model.pdf

[3] Waniczek 2022, Phd Thesis, System magazynowania energii w sprężonym powietrzu sprofilowany na potrzeby dużych jednostek wytwórczych.

[4] Bell F. G. et. all, Engineering in Rock Masses, Butterworth-Heinemann Ltd., Oxford 1992.

[5] Brady B. H. G. and Brown E.T., Rock Mechanics for Underground Mining, Kluwer Academic Publishers, Dordrecht 2004.

[6] Cundall P. A. and Hart R. D., Numerical modeling of discountinua, Comprehensive Rock Engineering, Vol. 2 – Analysis and Design Methods (C. Fairhurst, ed.), Pergamon Press, Oxford 1993, pp. 231 – 243.

[7] Cundall P. A. and Strack O. D. L., A discrete numerical model of granular assemblies, Geotechniqe 29, 1987, pp. 47 – 65.

[8] Hudson J. A. and Harrison J. P., Engineering Rock Mechanics, Pergamon – Elsevier Science Ltd., Oxford 1997.

[9] Jaeger J. C. and Cook N. G. W., Fundamentals of Rock Mechanics. Chapman & Hall, London 1979.

[10] Kirsch G., Die Theorie der Elastizität und die Bedürfnisse der Festigkeitslehre. Veit. Ver. Deut. Ing., 42, 1898.